



Probing low-energy electron induced DNA damage using single photon ionization mass spectrometry

Yanfeng Chen, Alexandr Aleksandrov, Thomas M. Orlando*

School of Chemistry and Biochemistry, Georgia Institute of Technology, 901 Atlantic Drive, Atlanta, GA 30332-0400, United States

ARTICLE INFO

Article history:

Received 1 April 2008

Received in revised form 19 June 2008

Accepted 9 July 2008

Available online 18 July 2008

Keywords:

Single photon ionization

Low-energy electron

Dissociative electron attachment

Dissociative ionization

DNA strand breaks

ABSTRACT

Single photon ionization mass spectrometry (SPI MS) followed by gel electrophoresis was developed for investigation of low-energy electron (LEE) induced DNA damage. This method detects neutral species generated from DNA molecules during LEE irradiation. The neutral yields are then correlated with single strand breaks (SSBs) and double strand breaks (DSBs) as a function of incident electron energy. Specifically, fragments with masses of $m/z=27$, 68 and 69 show resonance structure between 6–12 and 15–25 eV which is similar to that observed in the SSB and DSB probabilities. These fragments are likely associated with sugar damage and dissociative electron attachment (DEA) channels. Other fragments with masses of $m/z=45$, 56, 67 and 70 show a monotonic increase at threshold energies around 10–12 eV, indicating the possible role of direct dissociative excitation or ionization. Resonance structure above the 10–12 eV threshold for fragments with masses of $m/z=43$, 44, 67 and 70 are also observed and can be associated with compound states in the continuum and core-excited excitations. The results support the contention that DEA resonances localized on DNA sub-units can lead to damage, especially at energies below the ionization threshold. Damage also occurs due to direct dissociative excitation and dissociative ionization.

© 2008 Elsevier B.V. All rights reserved.

1. Introduction

Deoxyribonucleic acid (DNA) is one of the most important biological molecules for the survival of living organisms. DNA damage caused by radiation has been extensively investigated over the past several decades [1–8]. It is well known that high energy ionization radiation, such as α -, β -, X-, γ -rays, or heavy ions can cause sugar-phosphate cleavage (strand breaks) in DNA. Depending on the site of chemical bond dissociation, the DNA damage could be in the form of either a single strand break (SSB) or a double strand break (DSB). These lesions (particularly DSBs), if unrepaired, are likely correlated with toxic or mutagenic effects and cell malfunction or death.

Most of the energy deposited in living cells by ionizing radiation produces secondary species such as ballistic electrons (1–20 eV), neutrals, or ionic radicals [9]. Electrons are the most abundant secondary species with an estimated yield of about 4×10^4 electrons per MeV [10] and most of these secondary electrons have initial kinetic energies below 20 eV [11]. Pioneering work by Sanche and co-workers has demonstrated that low-energy electrons (LEE) can localize on various DNA components (nucleobases, deoxyribose, phosphate, or hydration water) to form transient negative

ions (TNI). The decay of the local transient anions into dissociating pathways, such as dissociative electron attachment (DEA) or autoionization, directly leads to DNA strand breakage [12–14]. The SSB and DSB yields as a function of incident electron energy have shown strong resonance features in the range of 5–15 eV with a maximum around 8–10 eV when irradiated by free ballistic electrons [12]. At higher energy, many non-resonant mechanisms and single/multiple ionizations can cause bond cleavage with a monotonic rising yield above the thermodynamic threshold [14].

Recently, the interaction of low-energy electrons with condensed films of DNA and substituent molecules (water, nucleobases, deoxyribose analogs and phosphate) have been investigated extensively [13–15]. For example, many previous studies on LEE interactions with DNA monitored resonance damage features by observing negative ion desorption [13] as a function of incident electron energy. Although negative ion (i.e., H^- , OH^- , and R^-) yields have been correlated to SSBs and DSBs, the DEA active sites were not identified because these negative ions could result from many different DNA components. Though there are only few reports that have focused on the detection of neutral products desorbing from DNA during LEE irradiation [13], the detailed physical and chemical processes leading to DNA damage can be better elucidated with this information.

The previous work on neutral detection during LEE irradiation of DNA films used electron-impact ionization quadrupole mass

* Corresponding author. Tel.: +1 404 894 4012; fax: +1 404 894 7452.

E-mail address: thomas.orlando@chemistry.gatech.edu (T.M. Orlando).

spectrometry (EI QMS) [13]. However, this method does not always generate molecular ions because most organic molecules fragment when ionized by the high energy electrons (70–100 eV) used in the EI process. Single photon ionization mass spectrometry (SPI MS) is a novel technique with special advantages regarding the detection of neutral molecules [16–18]. In this technique, pulsed or continuous vacuum ultraviolet (VUV) radiation sources with photon energies higher than 10 eV are typically used to ionize neutral molecules [19]. One commonly used SPI wavelength is 118 nm (10.5 eV). This is often produced via third harmonic generation (THG) using a high intensity pulsed 355 nm laser focused into a cell or jet containing xenon gas. Since the ionization potentials (IP) of most organic species range from 7 to 10 eV [20], SPI using VUV photons deposits less excess energy and favors the formation of parent molecular ions. This makes SPI a relatively non-selective soft ionization method for most neutrals [21] and a powerful tool for the observation of neutral products produced during the interaction of LEEs with DNA.

In this work, LEE induced DNA damage was investigated by monitoring the neutral yields as a function of incident electron energy using pulsed low-energy electron bombardment of DNA thin films and single photon ionization mass spectrometry. The SSB and DSB yields were determined as a function of incident electron energy using post-irradiation gel electrophoresis. Section 2 describes the experimental arrangement, Section 3 presents the neutral fragment yields and then correlates these with the SSBs and DSBs. A discussion regarding probable mechanisms involved in LEE induced damage of DNA is also given in Section 3. Finally, conclusions are given in Section 4.

2. Experimental method

2.1. Sample preparation

P14 double stranded circular DNA was derived from pBluescript SK II (–) (Stratagene, La Jolla, CA). It contains 6360 base pairs with a molecular weight of $\sim 4.2 \times 10^6$ Da. The plasmid DNA was further cleaned using Qiagen Maxi Prep kit (Valencia, CA) and the buffer and residual salts were removed by rinsing at least five times using nanopure water (18 M Ω). The purified plasmid DNA was resuspended in $1 \times$ TBE solution with a final concentration of 1 mg/mL verified by the UV–vis absorption spectrum. The DNA solution was then deposited on a 5 mm \times 5 mm Tantalum substrate, which was previously cleaned by acetone, methanol, and nanopure water with 10-min sonication period. The DNA sample was first held in a desiccator for 10 min and then moved into the loading chamber to be vacuum-dried. After about 24 h evacuation, the solid DNA film was transferred into the analysis chamber (UHV, 10^{-9} Torr) for low-energy electron irradiation experiments.

Our results, as well as others [13] using various substrates, indicate the biomolecules chemically decompose upon adsorption onto metal surfaces. Thus, we chose to study relatively thick (>5 monolayers) DNA films. The penetration depth/mean free path of 5–100 eV electrons is in the range of 15–35 nm in liquid water or amorphous ice [22]. The film thickness (>100 nm) assured that the measured signals were produced from electron interactions with the DNA molecules and prevented/minimized effects of back scattered electrons from the metal substrate. Since thick films could charge due to electron trapping, the potential build-up of charge was examined using a beam rastering procedure described below that allows routine imaging of the sample.

2.2. Electron irradiation

DNA solid films were irradiated at room temperature with a pulsed electron beam at various incident electron energies and fluxes. The pulsed electron beam was generated by a low-energy electron gun. The full-width at half maximum (FWHM) of the electron energy distribution was <0.5 eV. The focused beam size was 1–2 mm, depending on the electron energies. Irradiation of the sample (grounded or with an externally applied potential) was performed by the pulsed electron beam operated at 20 Hz with a 100 μ s pulse width. Variation of the electron flux was performed exclusively by changing the gun emission current. The electron flux was measured by picoammeter in the range of 10^{14} electrons $s^{-1} cm^{-2}$. The pulsed electron beam was focused on the target and controlled by x – y deflection to scan the entire substrate surface. When the electron interacts with the substrate or DNA, the image of the target (substrate or DNA) could be obtained by monitoring the voltage or current on the target. It was used to locate the DNA on the substrate and facilitated position control of the electron beam during irradiation. By using pulsed electron beam scanning, charging effects were greatly reduced. The total number of electrons exposed to the DNA molecules was on the order of 10^{15} with a 100 s scanning interval. The electron energy dependencies of the sample image quality taken over the 100 s scan indicated that charging did not occur.

2.3. VUV ionization and neutral detection

The neutral species produced and desorbed by low-energy electron irradiation of DNA molecules were ionized by VUV photons and detected by a quadrupole mass spectrometer (QMS), as shown in Fig. 1. The VUV photons (118 nm, 10.5 eV) were generated by frequency tripling 355 nm photons from a Nd:YAG laser in the THG cell filled with high purity xenon gas. The 118 nm photon intensity was optimized by increasing the 355 nm laser power and adjusting the xenon pressure. Since the VUV photon intensity depends on the Xe gas pressure, signals generated from neutral species during electron irradiation can be easily separated from background ions by doing experiments in the absence of Xe or simply turning the laser off. In this work, the 20 Hz 355 nm laser (~ 25 mJ/pulse) was focused into the tripling cell by a quartz lens (200 mm), and the xenon pressure was adjusted to ~ 8 Torr by observing the highest ionization signals from the neutral molecules. The VUV pulse energy was not measured but is expected to be approximately 0.01–0.1 μ J based on an approximate conversion efficiency of 10^{-6} to 10^{-5} reported in the literature [23,24]. To avoid multi-photon ionization due to the 355 nm laser, the 118 nm photons were separated from the 355 nm beam by taking advantage of the chromatic aberration of a LiF lens ($f=75$ mm for 118 nm photons) which also serves as a window. The distance between the sample surface and the 118 nm beam is ~ 1 –2 mm.

The electron beam incident angle was 45° with respect to the DNA surface. Neutral molecules that desorbed as a result of electron impact on DNA and ionized by 118 nm photons were detected by a modified QMS mounted perpendicular to the sample surface. An extraction plate was added to the QMS ion optics by applying a pulsed negative voltage after pulsed electron beam irradiation of the DNA film. The filament of the electron ionizer in the QMS was disconnected from the power supply to avoid fragmenting ions generated by VUV photons.

2.4. Post-irradiation gel electrophoresis

After electron irradiation, the DNA samples were removed from the chamber and re-dissolved in water. The amount of DNA was quantified by measuring absorbance at 260 nm before and after the

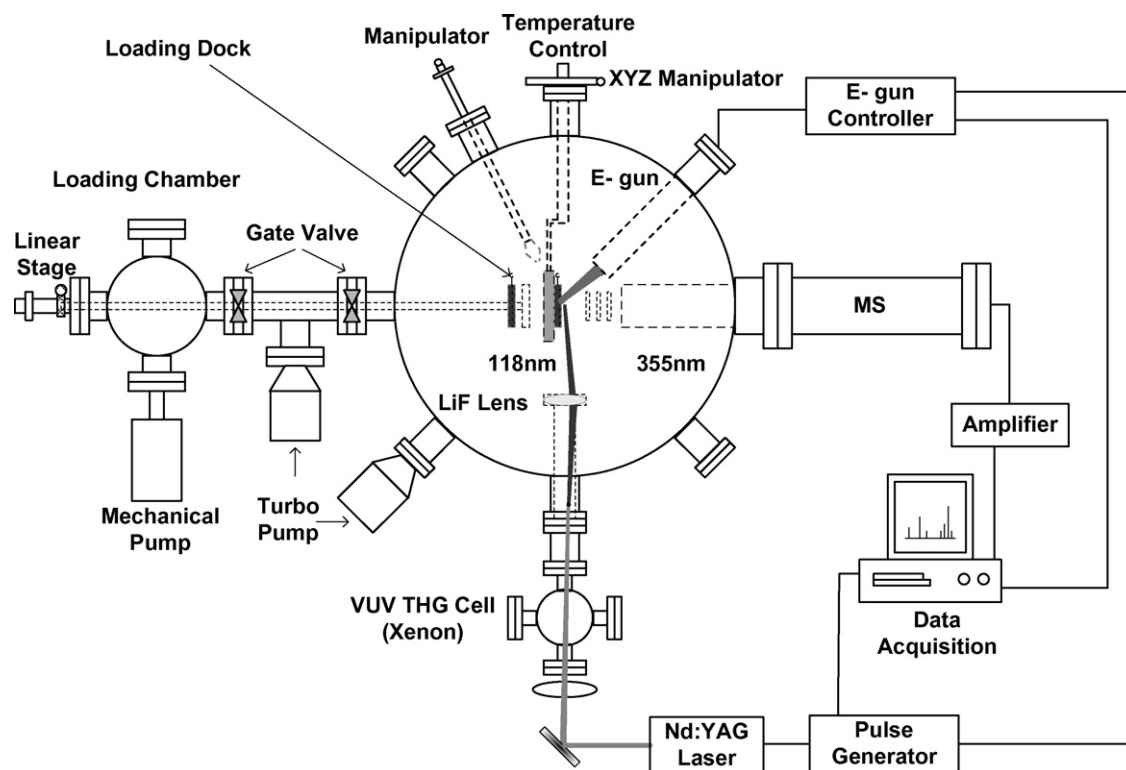


Fig. 1. Schematic of the single photon ionization mass spectrometer developed to study low-energy electron induced damage of DNA.

irradiation. Usually, more than 95% of the deposited mass of DNA could be recovered and the post-irradiated DNA samples (~ 200 ng) were analyzed by agarose gel electrophoresis. The supercoiled, SSB and DSB DNA could be separated by their different migrating abilities in agarose. Three controlled DNA samples were usually analyzed together with post-irradiation samples: (i) original plasmid DNA, (ii) a DNA sample that was dried, transferred in vacuum and recovered in water without irradiation, and (iii) DSB DNA made by the restriction enzyme *ScaI*. Quantitative analysis of SSBs and DSBs was carried out by integrating the light intensities of corresponding ethidium-stained DNA bands.

3. Results and discussion

3.1. SPI study of neutrals in LEE induced DNA damage

The neutral species generated during low-energy electron interactions with DNA molecules were detected by SPI MS. Fig. 2 shows the mass spectra of neutral molecules ionized by 118 nm photons at various incident electron energies. In Fig. 2, nine peaks specifically generated from DNA were detected in the mass range of m/z 20–75 when DNA films were irradiated by low-energy (5–25 eV) electrons at different energies. The neutral species can be tentatively assigned as fragments of DNA components (Table 1) based on NIST mass spectral library (v. 1.6) database searches and possible fragmentation pathways.

3.2. Post-irradiation analysis of LEE induced DNA damage by gel electrophoresis

As mentioned previously, after electron irradiation, DNA samples were analyzed by agarose gel electrophoresis. The quantitative SSB and DSB yields as a function of electron energy are shown in Fig. 3(a). The strand breaks were normalized by the amount of ana-

lyzed DNA and the number of incident electrons. The SSB yields are more than 10 times larger than the DSBs yields. This implies that most of the LEE induced damage is in the form of SSBs. It is also noticed that both SSBs and DSBs have relatively high yields around 10 and 20 eV. These resonant features are consistent with the contention that DNA damage by low-energy electrons can be caused by DEA channels (below 15 eV) and other excitation process (above 15 eV).

To allow detection of the desorbed neutral species, relatively high fluxes of electrons (10^{14} to 10^{16} electrons $s^{-1} cm^{-2}$) were used to irradiate the samples. This was also over a relatively long time (100 s) interval. Our previous work [25] reports a strand break (SSB, DSB and MDSB) yield of 10^{-3} using a dose of 10^{13} electrons/DNA film. Since we are now using at least 10^{15} electrons/DNA film, roughly 10% or more of the irradiated DNA form strand breaks. This is consistent with the observation that a smear pattern of multiple

Table 1
Neutral species detected by SPI MS in LEE induced DNA damage

m/z	Molecular formula	Possible source
27	HCN	Nucleobases
	C_2H_3	Nucleoside
43	$HCNO^a$	Nucleobases
	C_2H_3O	Deoxyribose
44	C_2H_4O	Deoxyribose
45	CH_3NO	Nucleobases
56	C_3H_4O	T
67	$C_3H_3N_2$	A, G
68	$C_3H_4N_2^a$	A, G
	C_4H_4O	Deoxyribose
69	$C_3H_5N_2^a$	A, G
	C_4H_5O	Deoxyribose
70	CH_2N_2O	T
	$C_2H_4N_3$	A, G
	$C_4N_6O^a$	Deoxyribose

^a Tentative assignment with lower probability.

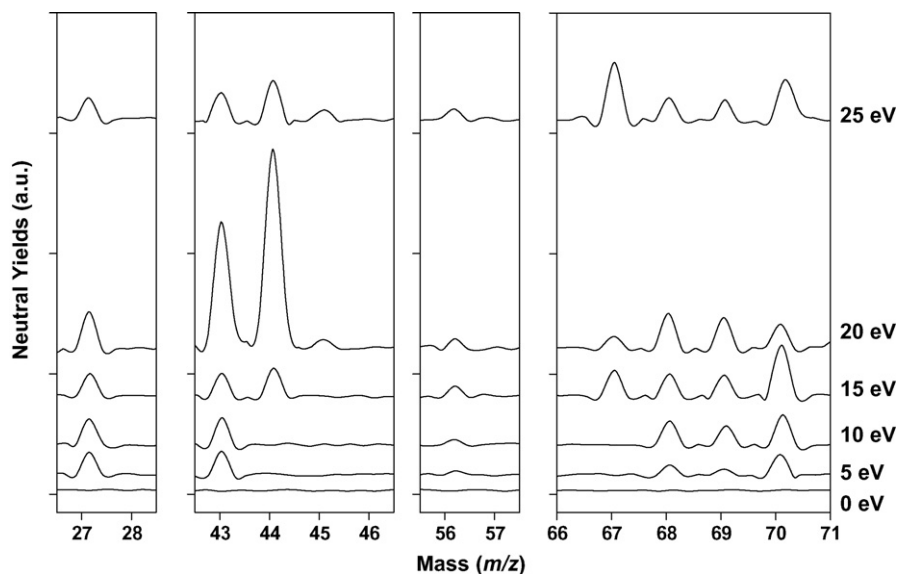


Fig. 2. Mass spectrum of neutral species produced and desorbed from P14 DNA as a result of low-energy electron bombardment and subsequent ionization by VUV photons. The incident electron energy, E_i , was increased at 5 eV increments.

strand breaks appeared in the energy range between 10 and 25 eV. Our fluence dependence measurements (not shown) also indicate that the dose used in our experiments (i.e., 10^{15} electrons/cm²) is not in the linear regime and that, in addition to DEA, multielectron impact processes are likely involved. Though this complicates the mechanistic analysis, the results are possibly relevant to hadron treatment and the hyperthermal-energy ion beam studies which result in locally high ionization rates and reactive scattering of

energetic fragments. It is important to note that the multielectron process can lead to multiple bond breakage and the possible excision of major neutral fragments of DNA. Potential mechanisms based upon multielectron processes and multiple bond breakage are discussed in more detail in Section 3.4.

3.3. Correlation between neutral species and LEE induced DNA damage

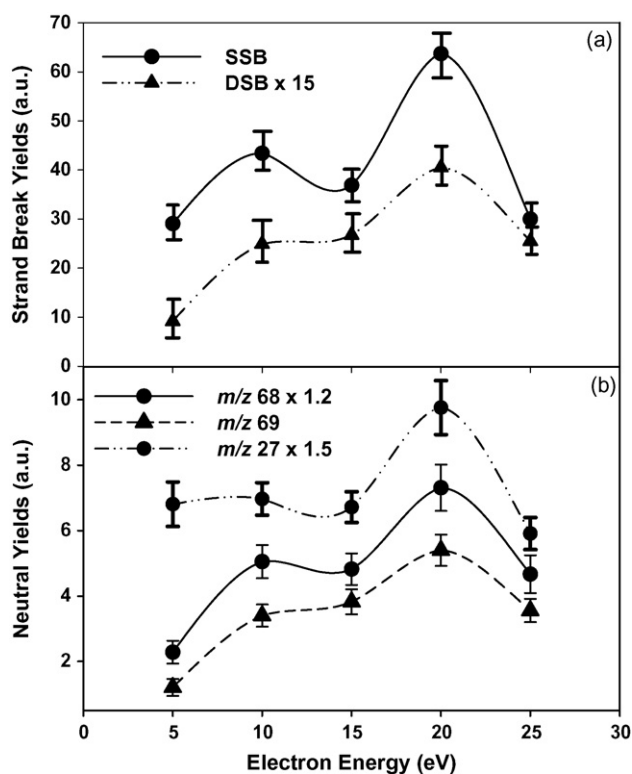


Fig. 3. DNA damage and neutral yields induced by low-energy electrons. (a) DNA single and double strand breaks determined by gel electrophoresis; neutral yields of (b) $m/z=27$, 68, and 69 from DNA under the irradiation of low-energy electrons (5–25 eV).

The yields of neutral species desorbed from DNA versus incident electron energy were compared to the corresponding SSB and DSB yields as a function of incident electron energy. In Fig. 3(b), the yield of $m/z=27$, 68 and 69 showed similar trends as the SSB and DSB probabilities shown in Fig. 3(a), indicating they may correspond directly with DNA damage. Since the resonance features of neutral yields of $m/z=68$ and 69 seem to fit the SSBs and DSBs, these two neutral species could be considered as good indicators of low-energy electron induced DNA damage. Indeed, Sanche and co-workers observed DEA resonances in condensed-phase deoxyribose analogues with peak energies around 10 and 20 eV [26]. The studies by Sanche monitored the H^- signal whereas the present work reports the probable neutral fragments of deoxyribose (C_4H_4O and C_4H_5O). Though fragments ($C_3H_4N_2$ and $C_3H_5N_2$) of the nucleobases can be formed, we favor the assignment of deoxyribose fragments. This suggests that DEA of deoxyribose is one of the major paths for electron induced damage of DNA. The 20 eV resonance features of $m/z=68$ and 69 could result from core excitations above the dipolar threshold which can support the formation of a transient anion that decays via DEA or autoionization. Finally, the neutral molecule at $m/z=27$ can also be correlated to SSB and DSB probabilities with resonance peaks at 10 and 20 eV, suggesting it is mainly desorbed from deoxyribose. However, its resonance shape between 5 and 15 eV is slightly different from that of SSBs and DSBs. Considering the possible contribution of DEA on nucleobase groups in DNA, the neutral molecules detected by SPI MS at $m/z=27$ could also contain some nucleobase fragments (HCN).

In Fig. 4(a) and (b), the intensities of other neutral peaks at $m/z=45$, 56, 67, and 70 were found to be dramatically different from the SSB and DSB probabilities shown in Fig. 3(a). These neutrals, therefore, were more likely generated from nucleobases rather than

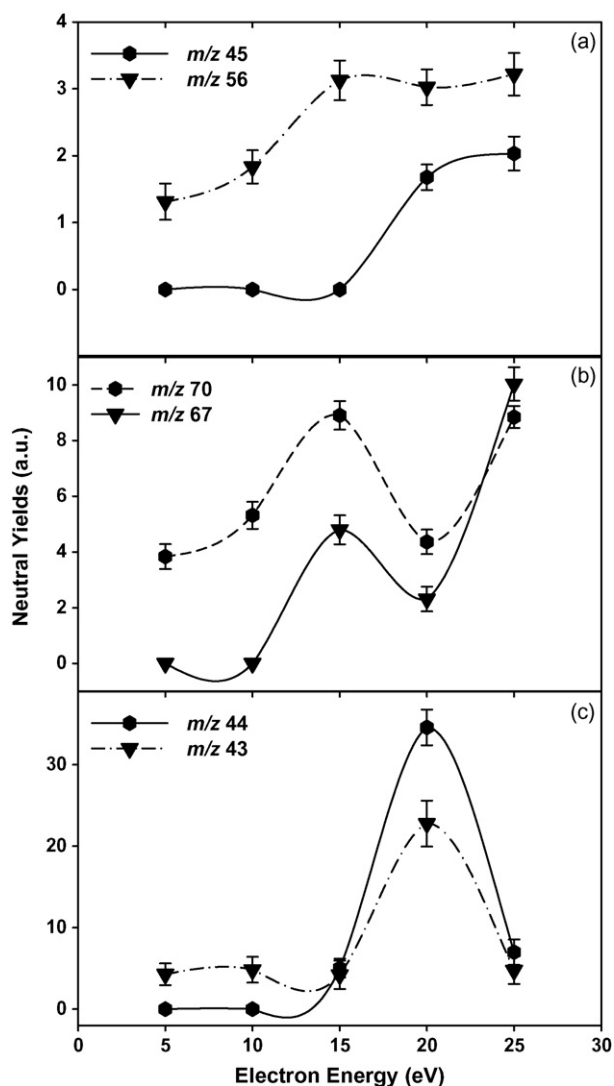


Fig. 4. Neutral yields of (a) $m/z=45$ and 56; (b) $m/z=67$ and 70; (c) $m/z=43$ and 44 from DNA under the irradiation of low-energy electrons (5–25 eV).

deoxyribose. The yields of $m/z=56$, 67, and 70 all displayed a resonance peak at 15 eV superimposed on a monotonically rising curve. This can be interpreted as direct ionization followed by dissociation from an electronically excited neutral state or direct dissociative ionization. The energy dependence of the $m/z=45$ yields demonstrated a typical single ionization curve with a threshold energy of 15 eV. Although these neutral products might be able to react further with DNA components to cause strand breaks through secondary pathways, Fig. 4 shows nucleobases can protect the DNA sugar moiety.

In Fig. 4(c), the neutrals of $m/z=43$ and 44 showed strong resonance peaks at 20 eV, which match the SSB and DSB resonance features at high energy. This indicates these two species could arise from deoxyribose through decay of a transient anion into a specific excited electronic state of nucleobases around 20 eV [26] followed by dissociation into reactive neutral species, leading to severe strand cleavage on DNA.

3.4. Mechanism of DEA related LEE induced DNA damage

Recently, several mechanisms of LEE induced DNA have been investigated by observing DNA fragments using high perfor-

mance liquid chromatography (HPLC) [27] and negative ion mass spectrometry [28,29]. Low-energy electrons can attach to nucleobase moieties, followed by charge transfer to the sugar-phosphate backbone, and induce phosphodiester bond breakage [27]. Low-energy electrons can also impact the phosphates in the backbone and produce OH^- via DEA to induce strand breaks [28]. In addition, DEA with resonance structure at 18 eV was found to lead to C–O bond cleavage by transient electron attachment to a σ^* anion state of the deoxyribose group, followed by dissociating into H^- and corresponding radicals [29].

In view of previous LEE DNA damage studies and these recent SPI MS results, generalized though somewhat speculative DNA damage mechanisms under high electron fluences are proposed based on several coincident pathways. These are shown as pathways (1)–(3) in Fig. 5.

We note that the primary waters of hydration are known to persist under our experimental conditions and have been correlated with DNA damage probabilities [25]. Therefore, we suggest that pathway (1) involves these waters of hydration. For example, a 10 eV incident electron can produce O , O^- , OH , and H^- via compound Feshbach resonances involving water and the DNA phosphates or possibly the bases. These same reactive species can also be produced at 20 eV via the 2-hole, 1-electron ($3a_1^{-1}1a_1^{-1}4a_1^1$) state [15] or possibly a core-excited resonance associated with a hole in the $2a_1$ level [30] of the structural water surrounding DNA [25,31]. Once produced, these radicals can lead to the formation of deoxynucleoside radical X (C3^*) by 3' cleavage [32]. The deoxynucleoside radical can then form an intermediate neutral molecule Y (2-base-2,3-dihydrofuran) through 5' cleavage [33]. Neutral molecule Y can finally undergo DEA or dissociation to desorb as the neutral products ($m/z=68$ and 69) detected by SPI MS. Another fate of molecule Y is to react with radicals or excited molecules created from the nucleobases or surrounding water to form neutral products ($m/z=68$ and 69). Note that the formation and ejection of the neutral sugar fragments is inherently a multistep, multielectron process.

Pathway (2) involves essentially the same sequence and intermediates. However, in pathway 2, a 10 eV electron can initiate damage by directly attaching to the deoxyribose group to generate the deoxynucleoside radical X (C3^*). The nucleobases in DNA molecules can also capture an electron and transfer it to the phosphate group [27]. According to theoretical calculations, electrons with incident energies <2–3 eV can cleave the C–O bond of the DNA backbone via an initial π^* transient anion, followed by transfer to the sugar. This transferred electron occupies the dissociative σ^* orbitals of the phosphates and can lead to efficient SSBs. DSBs require higher energy and may require an autodetachment/autoionization step and intrinsic hydration water [25].

Pathway (3) is invoked to help explain the resonance structure seen for $m/z=43$ and 44. At 18–20 eV, TNIs are formed by attachment to a σ^* anion state of the deoxyribose group [29]. This TNI then dissociates into the neutral deoxyribose radicals Z (C1^*). The deoxyribose radical Z can further decay to neutral compounds ($m/z=43$ and 44) and form radicals around the phosphodiester bond to cause strand breaks. Another possible path for DNA damage at 18–20 eV is multiple scattering electron energy loss (EEL) followed by resonance formation at lower energies (such as 10 eV) [14,34]. However, this process should generate a much stronger resonance damage peak at low energy [26], which is not supported by the data shown in Fig. 3. Therefore, multiple scattering electron energy loss may not be a dominant pathway for strand breaks in this study. In addition, the resonance structure at this high energy can be associated with direct Franck-Condon mediated dissociative

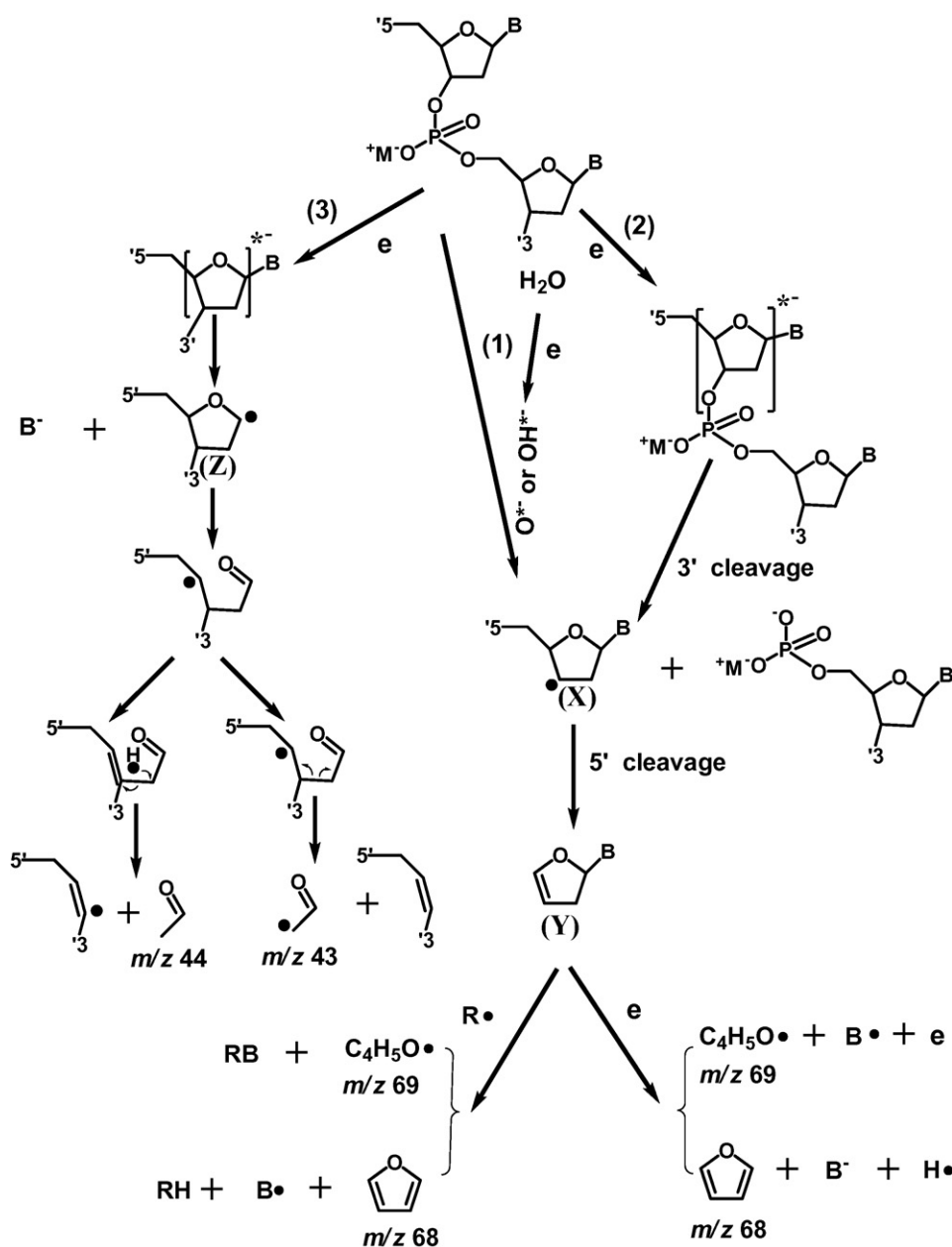


Fig. 5. Proposed generalized mechanisms of low-energy electron induced DNA strand breaks. The pathways discussed are likely to occur concurrently and involve multiple steps. The pathways are shown for the prominent neutral yields of $m/z=43, 44, 68,$ and 69 . The letter B represents the DNA base; R = radicals and M = counter ions.

excitation/ionization transitions to compound states in the continuum.

Based on the proposed mechanisms, it is concluded that low-energy electron induced DNA damage is a complicated process which involves different DNA components and surrounding water. When the electron energy is low (~ 10 eV), DEA on the deoxyribose group is likely one of the major causes of strand breakage. Although electron capture by nucleobases does not directly induce the DNA damage, it could facilitate the formation of TNIs by electron transfer to the phosphate-deoxyribose moiety. At higher energy (~ 20 eV), electrons interact with the deoxyribose group and surrounding water to produce strand breaks more effectively. The detection of the sugar related molecules ($m/z=43, 44,$ and 68 and 69) suggests that the deoxyribose radicals are involved in effective DNA damage.

4. Conclusion

Single photon ionization mass spectrometry followed by gel electrophoresis was developed for investigation of LEE induced damage of DNA plasmid films. Neutral fragments with masses of $m/z=27, 68$ and 69 show resonance structure between 6–12 and 15–25 eV which is similar to that observed in the SSB and DSB probabilities. These fragments are likely associated with sugar damage and dissociative electron attachment channels. Other fragments with masses of $m/z=45, 56, 67$ and 70 show a monotonic increase at threshold energies around 10–12 eV, indicating the possible role of direct dissociative excitation or ionization. Resonance structure above the 10–12 eV threshold for fragments with masses of $m/z=43, 44, 67$ and 70 are also observed and can be associated with compound states in the continuum and core-excited excitations. The

results support the contention that DEA resonances localized on DNA sub-units or compound states involving structural waters can lead to damage. Damage also occurs due to direct dissociative excitation and dissociative ionization. This technology/methodology is very likely to have broad applications in analyzing irradiation effects on other important molecules such as RNA and proteins.

Acknowledgements

This work was supported by the US Department of Energy, Contract DE-FG02-02ER15337. The authors thank Dr. Catherine Santai and Dr. Nicholas V. Hud for providing the DNA samples. We also thank Drs. Haiyan Chen, Christopher Lane, and Gregory Grieves for technical assistance.

References

- [1] S. Zamenhof, R. De Giovanni, S. Greer, *Nature* 181 (1958) 827.
- [2] G. Ahnstrom, *Mutat. Res.* 26 (1974) 99.
- [3] G.P. Van der Schans, A.A.W.M. Van Loon, R.H. Groenendijk, R.A. Baan, *Int. J. Radiat. Biol.* 55 (1989) 747.
- [4] M.A. Sognier, R.L. Eberle, Y. Zhang, J.A. Belli, *Radiat. Res.* 126 (1991) 80.
- [5] F.E. Ahmed, *Anal. Biochem.* 210 (1993) 253.
- [6] A.F. Fuciarelli, J.D. Zimbrick, Editors, Fourth in a Series of International Workshops held at the Salishan Lodge in Gleneden Beach, Oregon, October 1–6, 1994, 1995.
- [7] J.P. Banath, S.S. Wallace, J. Thompson, P.L. Olive, *Radiat. Res.* 151 (1999) 550.
- [8] B.P.C. Chen, D.W. Chan, J. Kobayashi, S. Burma, A. Asaithamby, K. Morotomi-Yano, E. Botvinick, J. Qin, D.J. Chen, *J. Biol. Chem.* 280 (2005) 14709.
- [9] C.V. Sonntag, *The Chemical Basis for Radiation Biology*, Taylor & Francis, London, 1987.
- [10] International commission on radiation units and measurements, IRCU Report 31, 1979.
- [11] V. Cobut, Y. Frongillo, J.P. Patau, T. Goulet, M.J. Fraser, J.P. Jay-Gerin, *Radiat. Phys. Chem.* 51 (1998) 229.
- [12] B. Boudaiffa, P. Cloutier, D. Hunting, M.A. Huels, L. Sanche, *Science* 287 (2000) 1658.
- [13] L. Sanche, *Eur. Phys. J. D* 35 (2005) 367.
- [14] M.A. Huels, B. Boudaiffa, P. Cloutier, D. Hunting, L. Sanche, *J. Am. Chem. Soc.* 125 (2003) 4467.
- [15] W.C. Simpson, M.T. Sieger, T.M. Orlando, L. Parenteau, K. Nagesha, L. Sanche, *J. Chem. Phys.* 107 (1997) 8668.
- [16] D.J. Butcher, D.E. Goeringer, G.B. Hurst, *Anal. Chem.* 71 (1999) 489.
- [17] O.P. Haefliger, R. Zenobi, *Anal. Chem.* 70 (1998) 2660.
- [18] M.J. Dale, R. Knochenmuss, R. Zenobi, *Anal. Chem.* 68 (1996) 3321.
- [19] P.D. Edirisinghe, S.S. Lateef, C.A. Crot, L. Hanley, M.J. Pellin, W.F. Calaway, J.F. Moore, *Anal. Chem.* 76 (2004) 4267.
- [20] D.A. King, *Surf. Sci.* 47 (1975) 384.
- [21] Y. Chen, M.C. Sullards, T.T. Hoang, S.W. May, T.M. Orlando, *Anal. Chem.* 78 (2006) 8386.
- [22] J. Meesungnoen, J.P. Jay-Gerin, A. Filali-Mouhim, S. Mankhetkorn, *Radiat. Res.* 158 (2002) 657.
- [23] T. Ferge, F. Muehlberger, R. Zimmermann, *Anal. Chem.* 77 (2005) 4528.
- [24] O.L.A.H. Kung, *Opt. Lett.* 8 (1983) 24.
- [25] T.M. Orlando, D. Oh, Y. Chen, A.B. Aleksandrov, *J. Chem. Phys.* 128 (2008) 195102/1.
- [26] D. Antic, L. Parenteau, L. Sanche, *J. Phys. Chem. B* 104 (2000) 4711.
- [27] Y. Zheng, P. Cloutier, D.J. Hunting, L. Sanche, J.R. Wagner, *J. Am. Chem. Soc.* 127 (2005) 16592.
- [28] X. Pan, L. Sanche, *Phys. Rev. Lett.* 94 (2005) 198104/1.
- [29] Y. Zheng, M.-E. Dextraze, P. Cloutier, D.J. Hunting, L. Sanche, *J. Chem. Phys.* 124 (2006) 024705.
- [30] G.A. Kimmel, T.M. Orlando, *Phys. Rev. Lett.* 77 (1996) 3983.
- [31] N.J. Tao, S.M. Lindsay, A. Rupprecht, *Biopolymers* 28 (1989) 1019.
- [32] A. Adhikary, A. Kumar, M.D. Sevilla, *Radiat. Res.* 165 (2006) 479.
- [33] A. Adhikary, D. Becker, S. Collins, J. Koppen, M.D. Sevilla, *Nucleic Acids Res.* 34 (2006) 1501.
- [34] D. Antic, L. Parenteau, M. Lepage, L. Sanche, *J. Phys. Chem. B* 103 (1999) 6611.